Katrein Sauer[a], Alexander Rack[b], Hawshan Abdulrahman Mustafa[c], Mario Thiele[a], Ron Shahar[d], Paul Zaslansky[a,c]

[a] Julius Wolff Instiut, Charité – Universitätsmedizin Berlin, Germany
[b] ESRF – The European Synchrotron, Grenoble, France
[c] Department for Operative and Preventive Dentistry Centrum für Zahn-, Mund- und Kieferheilkunde, Charité – Universitätsmedizin Berlin, Germany
[d] Koret School of Veterinary Medicine, The Robert H. Smith Faculty of Agriculture, Food and Environment, The Hebrew University of Jerusalem, Rehovot, Israel

Microstructure and texture contributing to damage resistance of the anosteocytic hinge-bone in the cleithrum of *Esox lucius*

Paper presented at the Symposium "Tomographic and Radiographic Imaging with Synchrotron X-rays and Neutrons" of the MSE 2018, 26–28 September 2018, Darmstadt, Germany

Bones are nanocomposites of protein, mineral and water that form mineralized collagen fibrils arranged in a variety of layered lamellae. Bone material has a long evolutionary record and specific bones attain shapes and microstructures that have well stood the test of time such that they can be considered optimized to match their function. Further, most bones typically contain entombed living cells, osteocytes responsible for adaptation, healing and biochemical signaling. The bones of pike fish (*Esox lucius*) are different because, as with other advanced teleost species, they evolved to eliminate osteocytes from the microstructure. This suggests that these cells are not needed because these bones are more damage resistant than mammalian bones. Here we explore details of this biologically-grown structure, using a combination of light and X-ray based characterization methods. We report the three-dimensional arrangement and composition of the heavily cyclically-loaded pivot of the cleithrum bone in the pectoral girdle of pike. By combining absorption and phase contrast-enhanced micro-computed tomography, electron microscopy, polarized light microscopy and second harmonic generation multi-photon confocal laser scanning microscopy we reveal the principle layout of the bone of this predator which we determine at the millimeter, micrometer and nanometer lengthscales.

Keywords: Pike bone; Mineralized collagen fibril; microCT; SHG confocal imaging; BEI electron microscopy; Cyclic loading

1. Introduction

Bones are made of biocomposites of stiff nanoparticles of hydroxyapatite embedded in strong collagen protein fibers and water. Usually, typical mammalian bone contains entrapped, metabolically-active cells (osteocytes), linked by a mesh of connecting tentacles (canaliculi). The integration of living cells into the bone matrix is considered to be essential for the normal function and biological responsiveness of bones, especially under variable mechanical loads, where adaption or healing (remodeling) remove damage-accumulation. But living cells are energetically expensive, and some evolutionarily advanced fish known as 'advanced teleosts', evolved bones devoid of osteocytes. The lack of living cells does not mean that the bone material is 'dead': on the contrary, recent reports clearly show adaptation, healing and remodeling without osteocytes, for example in tilapia [1] or the rostral bills of swordfish and marlins [2]. The thin wing-shaped cleithra of the rapacious northern pike (*Esox lucius*) are interesting examples of heavily loaded anosteocytic bones since they endure frequent repeating stress cycles and they function for many years. These bones serve the ambush-feeding habits of this fresh water large predator [3] that populates the northern hemisphere lakes and rivers. The anchor-point of these bones, the pivot, functions as a hinge undergoing compression and perhaps some bending. Away from the pivot, the cleithra are attached to many powerful muscles that cyclically and rapidly actuate mastication, whenever unlucky prey is devoured. These bones form a mobile frame for the head wall [4] for stabilization and protection purposes, and they support and anchor the pectoral fin [5] (Fig. 1a, b). During predation, rapid expansion of the head is induced by rotation of the cleithra bones around their stout thickened pivots. It is assumed that the pivot is pushed against the supracleithrum (scl) during every contraction cycle of the large, strong musculature [6] (Fig. 1).

Repeated cyclic loading is challenging to any mechanically loaded structure, and questions arise as to how exactly the cleithrum microstructure matches the feeding habits of the relatively long living pikes. While much remains unknown about the details of the stresses and strains involved, it is clear that significant forces and bending moments are involved. The cleithrum thus needs a resilient pivot to endure anteroposterior as well as dorsoventral stress [7].

Previous work on analyzing cleithra structure has focused on practical needs to determine the fish age [8, 9], to identify specific species [4], or to estimate rate of growth [10]. Yet it is well known that adaptation of bone tissue to match function occurs at a macroscopic (millimeter) as well as at the fiber-array (micrometer-nanometer) length-scales [11]. Osteoblast cells typically produce bone whereas osteoclasts remove unwanted tissue, and in mammals, osteocytes orchestrate and control this remodeling process. However, pike only have osteoblasts and osteoclasts, which in the field of bone biology would suggest that these bones cannot adapt structurally to external mechanical loads. It is thus unclear whether pike bones indeed have the capacity to adapt to external loads.

The contribution of preferred mineralized fiber orientations and their distribution to the mechanical competence of bones have been the subject of extensive research [12]. In fact, bone texture is often indicative of the loads to which it is subjected. Indeed, fibers oriented along the bone axis of long mammalian bones are thought to better resist tensile forces [13], fibers oriented transverse to the long bone axis are 'optimized' to resist axial compressive forces [14] whereas fiber arrangements along diagonal orientations (e. g. 45 degree rotated plies as in the case of bone lamella in long bones), are well suited to supporting and resisting preferential shear forces [15].

To date, little is known about the relationship between the mechanical loading scenarios and the micro–macro structural arrangement of the mineralized collagen fibrils in anosteocytic bone such as the pike cleithra. In this paper, we combine both wet and dry imaging methods utilizing µCT (Micro-Computer Tomography), electron and light microscopy methods, to characterize and map the principle architecture and micro-morphology of anosteocytic fish bone, as a foundation for future structure–function relation studies in such bony structures.

2. Materials and methods

2.1. Sample preparation

Cleithrum samples were dissected from different Esox lucius specimens, collected from $n = 5$ recently-caught fish, purchased in local fish markets in Berlin, Germany. Four different sample preparation approaches were used for macroscopic architecture, mineral density and collagen fiber orientation studies. For overall geometry and density analysis large segments of the cleithrum pivot ($\sim 6 \times 6 \times 10$ mm, Fig. 1c) were cut with a slow speed precision water-cooled saw (IsoMet, Buehler, ITW Test and Measurement GmbH, Düsseldorf, Germany) using a diamond wafering blade. These samples were used for full thickness µCT imaging. Native, wet, longitudinal and transversal sections were used for imaging by light and confocal laser scanning microscopy with second harmonic generation (SHG). Some of the samples were ground successively with increasing grit-sizes and emery sheets, polished with diamond suspensions with grain sizes of 3 µm, 1 µm and 0.25 µm for scanning electron microscope (SEM) backscatter electron imaging (BEI) and energy dispersive X-ray spectroscopy (EDX) chemical mapping. These samples were then air dried before carbon coating (MED010 Balzers union, Wiemer EM-Service oHG, Wetter, Germany). Other slices were demineralized by bone embedding procedures for collagen fiber imaging. Standard processing included decalcification by immersion in EDTA for 9 days with solution changes every 3 days, followed by dehydration in a graded series of alcohol solutions in an automatic tissue processor (Leica TP1020, Leica Biosystems Nussloch GmbH, Nussloch, Germany). Decalcified samples were embedded in paraffin and cooled for slicing with a microtome (LEICA RM2235, Leica Biosystems Nussloch GmbH, Nussloch, Germany) to produce 5 µm thick slices. Samples were then deparaffined with Xylol, rehydrated in a descending alcohol series starting at 100 %, 96 %, 80 % down to 70 %, in preparation for staining. Picrosirius red powder (Direct Red 80, Sigma – Aldrich 365548) was solved in Picric acid and flushed with acetic acid, ethanol and Xylol. The samples were placed on microscope cover glass and coated with mounting media (Vitro-Clud, R. Langenbrick GmbH, Labor- und Medizintechnik, Emmendingen, Germany) in preparation for imaging.

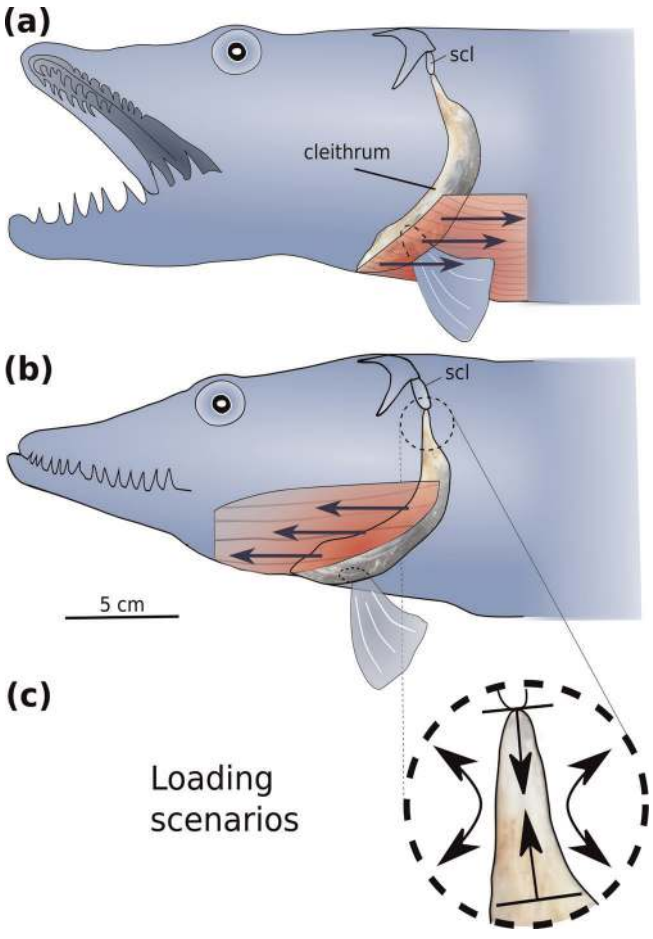

Fig. 1. Forces acting on the cleithrum bone within a pike fish (*Esox lucius*), indicated as a result of muscle contraction: (a) Following mouth opening, and (b) mouth closing during prey capture. Due to the attachment of the pectoral fin to the cleithrum, additional pressure is exerted on the cleithrum bone. (c) Loads from the muscles and the pectoral fin actuation lead to increased loading, presumably bending and compression within the cleithrum and up to the pivot point (black dashed circle). Both bending [7] and compression involve interaction with the attached supracleithrum (scl) in a dorsal direction.

2.2. Structural characterization

2.2.1. Tomographic imaging

Native samples were scanned by both lab-based μCT (Skyscan 1172, Brucker-microCT, Kontich, Belgium) and synchrotron μCT in absorption and phase contrast modes (ESRF, Grenoble, France [16]). Lab-based μCT image voxel size was 2 μm and scans were conducted using a source energy of 80 kV (source current of 124 μA). These scans were reconstructed with NRecon (Version 1.7.0.3, Bruker microCT, Kontich, Belgium) and visualized using CTVox (Version 3.3, Bruker microCT, Kontich, Belgium). Synchrotron data were collected on beamline ID19 of the ESRF, with a photon energy of 34 keV and an image pixel size of 0.65 μm. Scans were performed on both wet (in sealed vials) and air dried samples. Inline phase contrast enhancement was used employing propagation distances of 22 and 88 nm between sample and detector. The large (>4000 projections) data sets were reconstructed using the open-source code *PyHST2* [17] and single-distance phase-retrieval data was reconstructed with a delta–beta parameter ratio of 500, similar to previous protocols [18]. Cropping and visualization were performed using Fiji [19].

2.2.2. Second harmonic generation confocal laser scanning microscopy (SHG)

Both native as well as decalcified sections were imaged to visualize collagen fiber orientations and distributions. SHG (Leica TCS SP5II confocal microscope, Leica Microsystems GmbH, Wetzlar, Germany) was performed using a water lens (Leica HCX IRAPO L 25.0 × 0.95) using a pinhole of 600 μm. Samples were imaged wet with a lateral resolution of approximately 600 nm and a voxel (step) height of approximately 500 nm. Stacks consisted of 60 or more images were scanned and the 3D images were visualized and analyzed with Fiji.

2.2.3. Electron microscopy: backscatter imaging and EDX

Carbon coated samples were scanned with SEM (CamScan MaXim, Electronen-Opti-Service GmbH, Dortmund, Germany) using an acceleration energy of 20 kV. EDX spectra were collected (QUANTAX EDS XFlash 6130, Bruker Nano GmbH, Berlin, Germany) and processed (Esprit 2.0, Bruker QTX, Berlin, Germany) to determine Ca counts using a dwell time of 256 μs and a line average of 6 with a ∼1 μm spot size.

2.2.4. Polarization light microscopy

Picrosirius red stained samples were imaged using a polarization light microscope (Leica, DMRB 019095, Leica Microsystems GmbH, Wetzlar, Germany) with defined orientations of the samples with respect to the crossed polarizers. To highlight the structural orientation we took advantage of the birefringence of the collagen fibers visible when linear polarized light propagates through the dye molecules attached to the collagen fibers [20]. Images of the histological thin demineralized stained sections were taken at angles 0°, 45°, 90°, 135° 180°; with a pixel size of 0.75 μm. Rotating the sample in-plane by 90° reveals intensities that are equivalent to those observed 0° and 180°. The images were superimposed using the ImageJ [19] 'Registration' plugin.

3. Results

3.1. Overall morphology

Standard μCT showed that the cleithrum pivot has a rather uniform density yet it contains rather large, hollow, elongated cavities oriented axially. Figure 2 shows a typical reconstruction with the internal spaces, possibly marrow chambers, exposed in the 3D rendering. It can be seen that large voids cluster near the central regions of the bone, seemingly hollowing it out so as to minimize redundant material, while ensuring sufficient support with vertical "pillars" to prevent compression or bending over-load.

3.2. Lamellated, wavy, bone layers

The cleithra pivot is characterized by extended regions of layered lamellae with low and high densities. Figure 3 shows typical 2D cross-sections directly comparing the complementary imaging methods we used for the same bone region (Fig. 2). The μCT reconstructed slice (Fig. 3a) shows two main bone architectures: a central zone, filled with large voids and a rather uniform compact outer shell (cortex) of a seemingly uniform density material (partly marked with a dashed square). In some regions large voids are seen, some irregularly shaped. Other regions exhibit a myriad of small uniform voids/channels. Additional detail becomes evident by

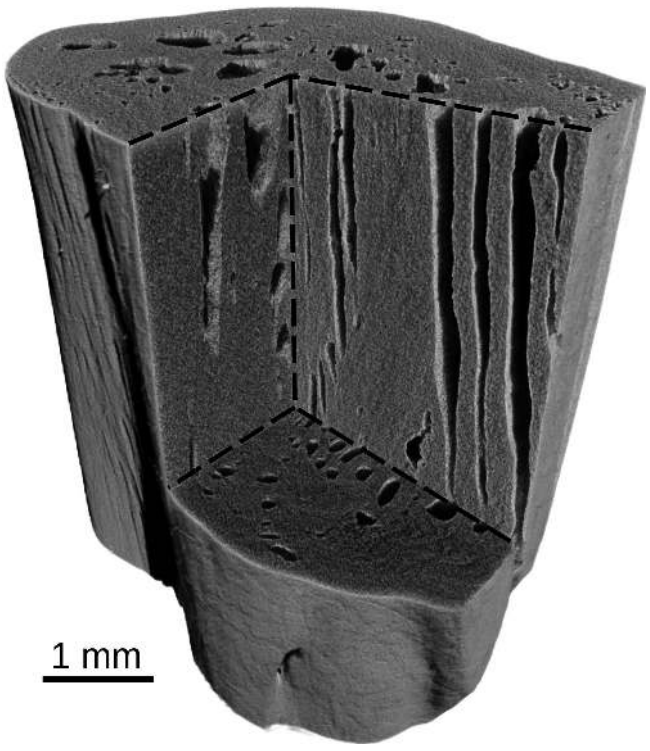

Fig. 2. Laboratory μCT 3D reconstruction with a voxel size of 2 μm provides views into the cleithrum pivot as outlined in Fig. 1c. The dense mineralized collagen matrix is centrally hollowed-out with large channels which contain blood vessels and living tissue.

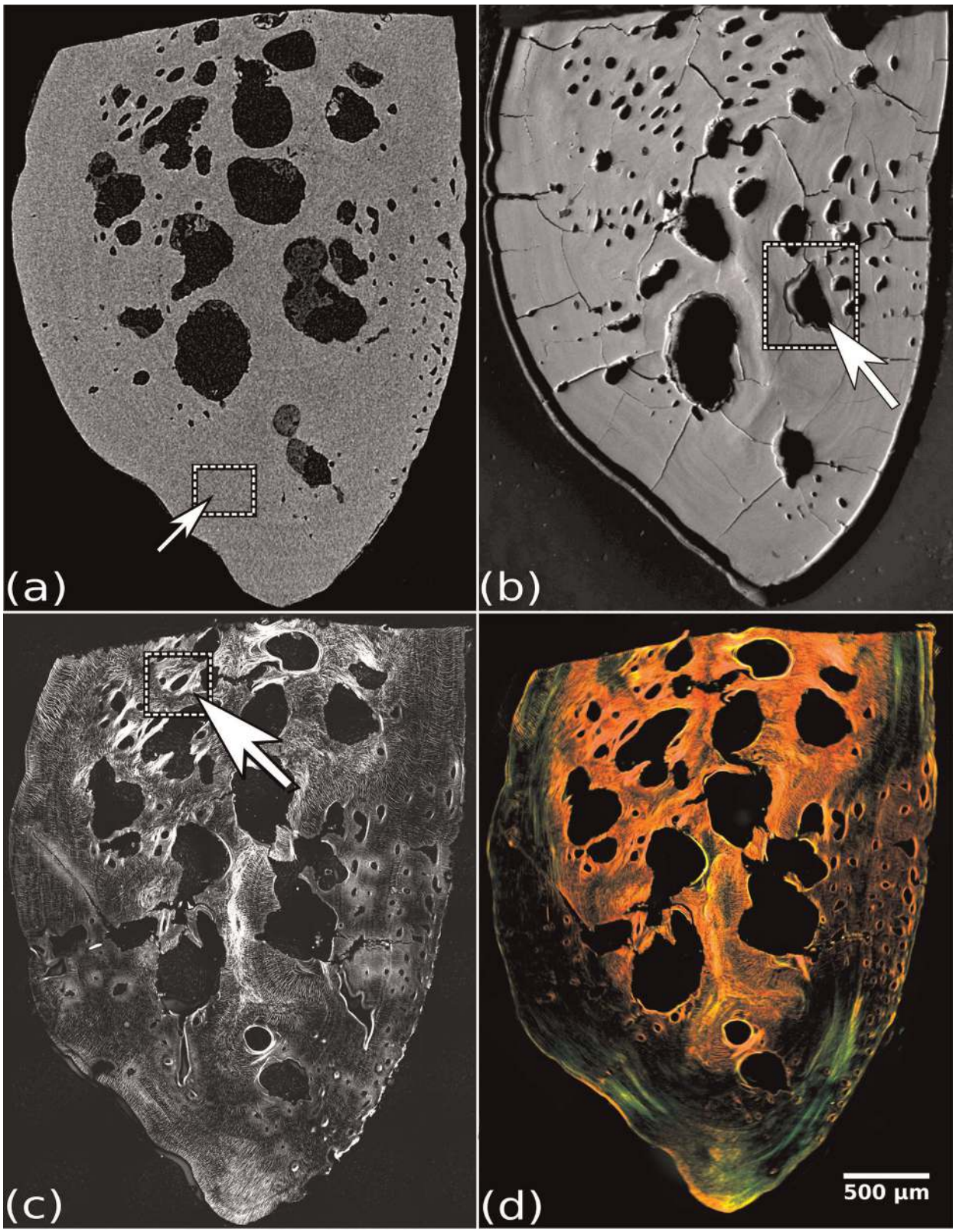

Fig. 3. Cross-section of a typical cleithrum pivot (Fig. 2, top view) showing comparison between signals obtained from four complementary imaging methods: (a) laboratory µCT shows the compact mineralized matrix (for example the dashed square marked with a white arrow) with incorporated huge channels in the center of the pivot, some exhibiting erosion or resorption zones. (b) BEI imaging by electron microscopy where erosion zones are visible (see dashed square with a white arrow). (c) Second harmonic generation (SHG) images show the signal arising from collagen fibers with a variety of motifs seen across the entire bone section (white arrow shows an example for collagen fibers surrounding one of the channels, shown at higher magnification in Fig. 5). (d) Polarization light microscopy of a demineralized thin section reveals the collagen stained with Picrosirius red, with different densities and orientations seen throughout the cross-section of the cleithrum pivot. The colors correlate with fiber thickness: there is an increase in thickness as the color changes from green to yellow to orange to red, see [10].

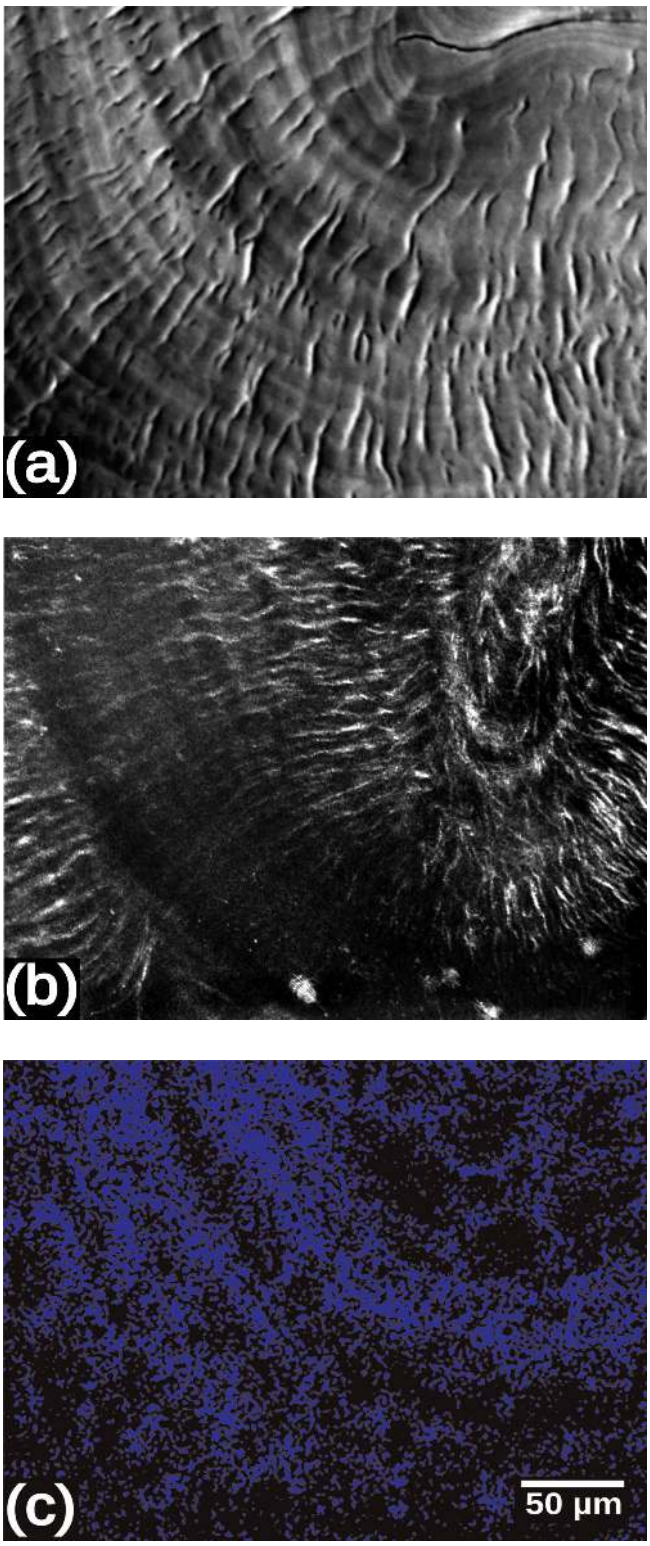

Fig. 4. High resolution images of dense and compact bone regions (marked with a square in Fig. 3a) show (a) collagen fibers (radiating wavy patterns) are seen perpendicular to the large number of parallel layers, exhibiting slight density variations between adjacent lamellae. (b) Collagen fiber distribution by SHG (white). (c) Calcium distribution (blue) by EDX.

BEI where the high energy scattered electrons reveal layers as well as small density variations in the bone mineral (Fig. 3b). The periphery of some of the voids shows evidence of resorption, and some are partially lined with less-dense material (remains of organic living matter), closely associated with zones of internal 'erosion'. The main signal in the BEI images correlates with the atomic number of the elements in the structure, which is dominated by Ca due to the relatively high atomic weight of calcium in the mineralized matrix. This shows stark contrast with the bright collagen signal, obtained by SHG (Fig. 3c). Various fibril motifs are visible, including radiating or parallel fibril arrays. Some of the larger central voids are surrounded by layers of radial dense fibers. Thus, it is seen (compare rectangles in Fig. 3b and c) that some voids are surrounded by reinforcing multiple layers of collagen, while others are not, presumably in the process of being removed by osteoclast cells lining the voids internally. Similar observations are seen in demineralized sections observed by polarization light microscopy (Fig. 3d) of decalcified tissue. The collagen matrix signal reinforced by the Picrosirius red stain, indicates that there are different collagen fiber orientations and even a varying fiber thickness, identifiable by the red versus green regions in the central and outer bone zones. Color changes from green to yellow to orange to red suggest an increase in fiber thickness [20]. Note that the slice thickness is uniformly 5 µm.

3.3. Compact mineralized collagen fiber mesh

A closer look at the microstructure of the outer compact bone (marked by the rectangle in Fig. 3a) reveals an interconnected mesh of collagen fibers, permeated with mineral (see Fig. 4). Direct comparison of cross-sections by BEI, SHG and EDX reveals clearly visible layers of bone material with variable density and layer thickness. Comparison between the BEI, SEM and SHG images (compare Fig. 4a and b) suggests that layers of dense mineral are orthogonally pinned together with low-density collagen fibers. Pinning is achieved by fibers traversing multiple layers and is seen by small, outward-radiating wavy lines that are collagen fibers. Note how the BEI and SHG signals of the layered mineral density (concentric like semicircles) inversely match the collagen arrangements. Indeed, Ca distribution, measured with EDX (Fig. 4c), nicely correlates with the higher mineral density layers obtained by the BEI method (Fig. 4a).

3.4. Structural motifs of the mineralized collagen fibers

By combined use of the complementary methods, we observe two different structural motifs. High resolution images of the enlarged sections of the channel walls are depicted in Fig. 5 revealing texture lining the internal voids. SEM and SHG images of smooth, oval-shaped voids depict gradual transitions from the rim into the surrounding mineralized matrix (a) with clear, well defined enclosing collagen fiber arrays (b); eroded layers of material are seen in some internal voids, where both the mineralized matrix (c) and the collagen arrays (d) are removed presumably by osteoclast cells. Note that cracks seen in (c) are drying artifacts, visible in the SEM image only, as are the bright 'charging artifacts'. We conclude that in some of the channels, the matrix is resorbed, with partial removal of the bone material, reminiscent of mammalian bone modeling.

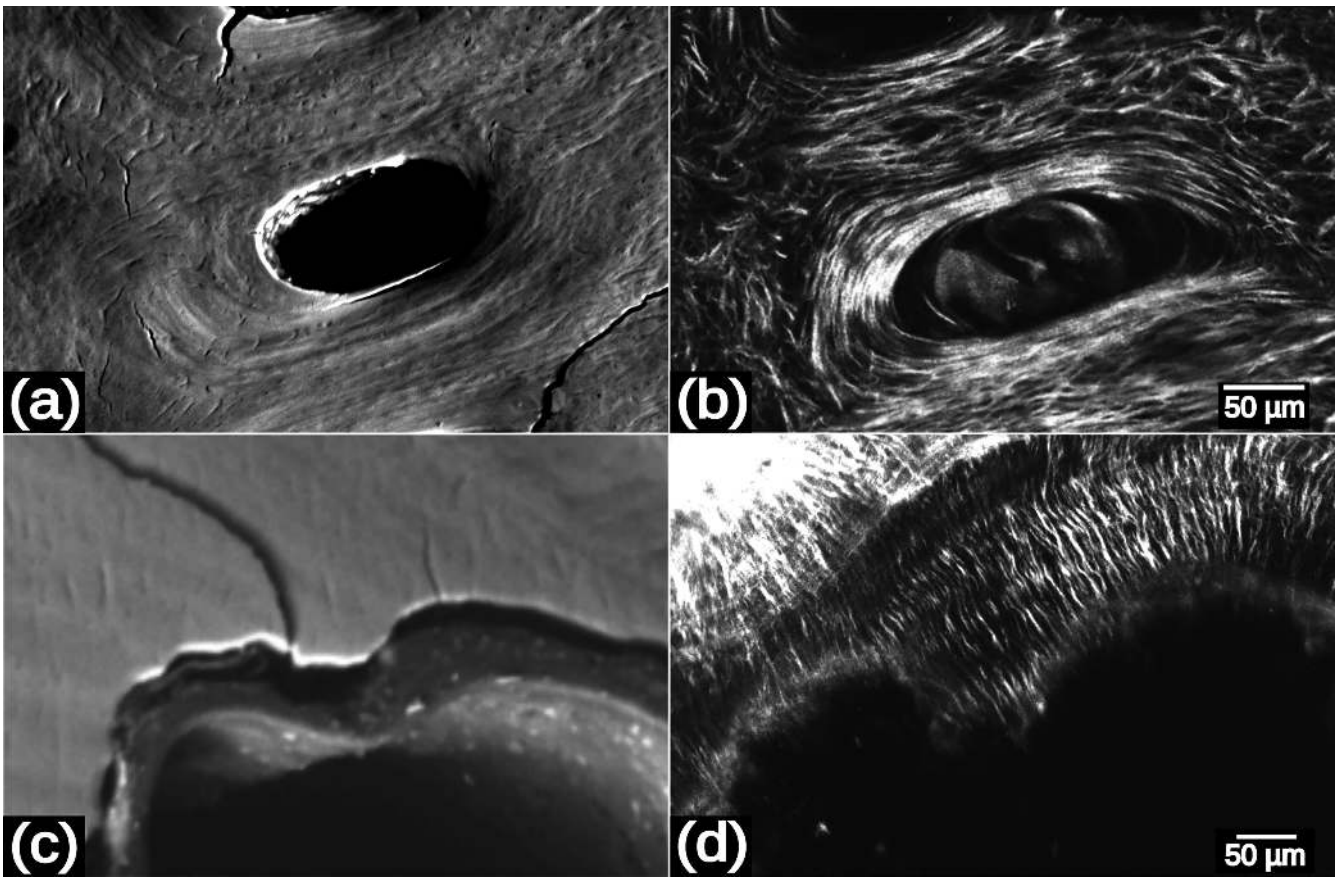

Fig. 5. High resolution cross-sections of pores in Fig. 3b and c revealing the microstructure surrounding central region of the cleithrum pivot. Two different structural motifs are observed: (a) Mineralized collagen fibrils encircling the channel, as observed with backscattered electron imaging (BEI) microscopy. (b) Collagen fibers visible by second harmonic generation (SHG) confocal laser scanning microscopy where fibers are seen to surround the channel. (c) BEI, and (d) SHG images also demonstrate channels exhibiting internal resorption. Vessel edges appear eroded from the inside with clear evidence of bone removal by the bone-resorbing cells in the cavities. Cracks in the BEI images (a) and (c) are due to drying artifacts.

3.5. Phase contrast-enhanced µCT

Mineralized collagen distributions of both cross-sectional and longitudinal views of the cleithrum pivot are shown with high-contrast high-resolution synchrotron phase contrast enhanced Paganin reconstructed images [16]. As shown in Fig. 6a–d, layers of slightly-varying mineral density (not visible in absorption µCT scans) form the backbone of the entire structure, appearing as juxtaposed plies of a composite. Intensity undulations are seen in the cross-sectional view (a) and the enlarged zoomed-in image (Fig. 6b) reveal layers of higher density amid layers of lower density, possibly indicating recently deposited bone. Some cavities nicely exhibit regions of bone-tissue removal, presumably as part of the biological process of bone modeling. The same layered structure is seen in longitudinal orientation (Fig. 6c) with a magnified view shown in (Fig. 6d). Here, extended layers are seen along the long axis of the internal cavities, where the channels run along the pivot axis. SHG (Fig. 6e) confirms the existence of a longitudinal collagen fiber motif. Both orientations observed in virtual slices in the µCT data in cross-sectional and longitudinal directions reveal cut-out bony regions, where some of the bone is apparently removed from within the cavities. Curiously, within the longitudinal magnified slice (Fig. 6d) both dense, well arranged mineralized collagen layers as well as loose, disordered zones in the matrix material appear to be in the process of removal. Bone adaptation in pike is thus not limited to old, damaged bone.

4. Discussion and conclusions

Our results highlight the main structural motifs in the thick supporting pivot of the pike cleithrum, which we mapped at the mm, µm and nm length-scales. We observe a laminated pattern of bone layers that appear to be pinned together by poorly-mineralized orthogonally-directed collagen bundles. The bones also show evidence for adaptation through modeling, i. e. bone tissue removal and deposition at different locations by living tissue, presumably osteoclasts, located in large internal cavities. These cavities populate the central region of the bone, reducing the overall mass. The existence of cavities in the center leads to only a minor decrease in the resistance to bending, while significantly reducing the weight of the bone, a common engineering principle frequently found in both man made [21] and in natural structures such as the long bones of mammals. It also allows for the passage of blood vessels into the bone. We find that the pivot structure is designed to form a strong foundation, well capable of sustaining repeated loads by making cunning use of multiple

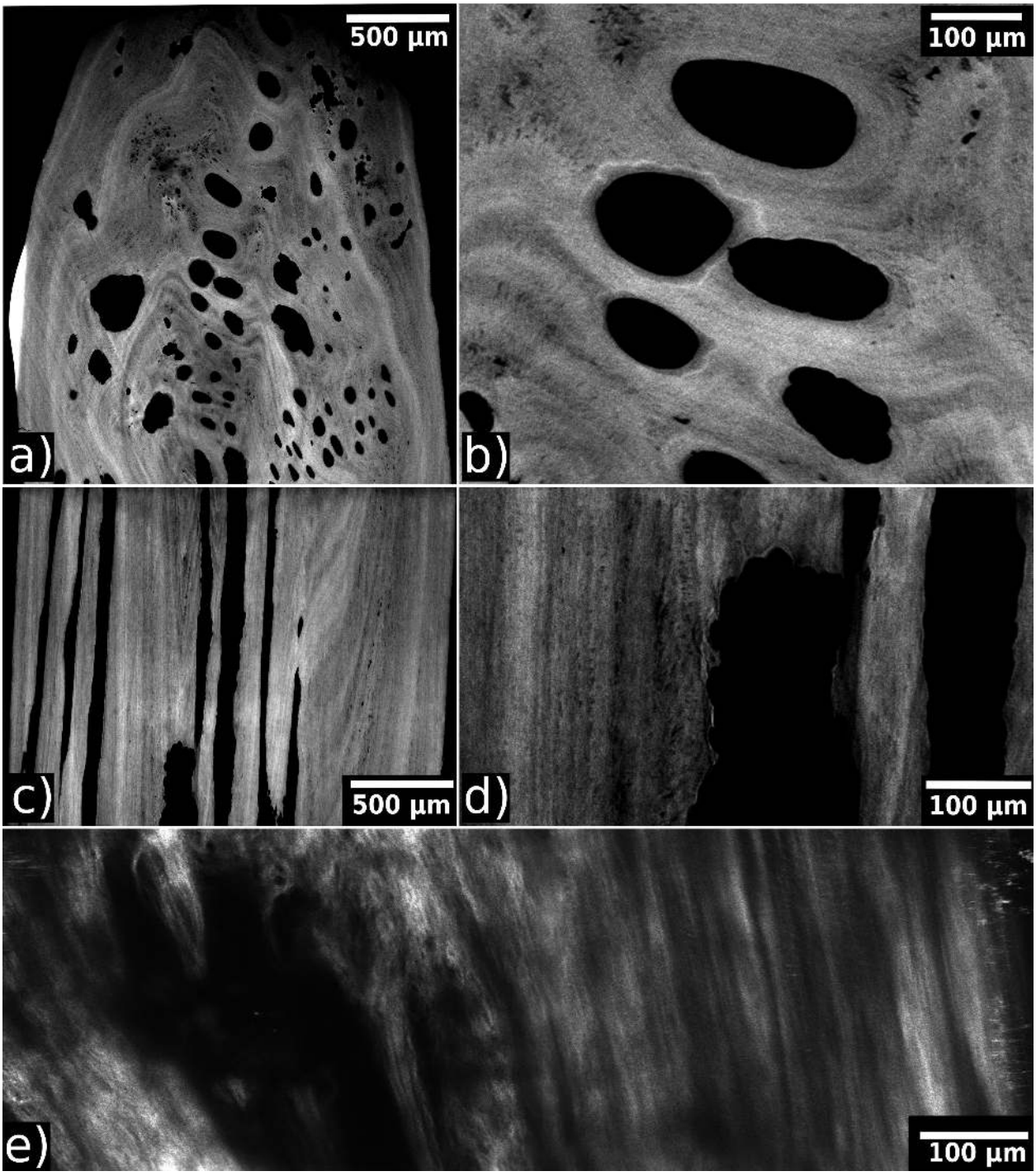

Fig. 6. High resolution synchrotron phase contrast enhanced µCT images show (a) cross-sectional views of the cleithrum pivot comprising variable density layers. (b) Enlarged details of (a). (c) Longitudinal view of cleithrum pivot, and (d) an enlarged detail of (c). e) High resolution longitudinal SHG image shows the contribution of many layers of co-aligned fibers.

layers. It is strengthened on the micrometer scale by transversally cross linking fibers, that pin adjacent layers together, resisting delamination or cracking due to axial compressive forces. Such a design is well able to handle cycles of compression loading, since the composite strength is the greatest when the fiber bundles are oriented transversally to the axial compressive forces [14].

Anosteocytic bones are different from the bones of mammals, including human bone [22]. In pike (*Esox lucius*), despite repeated loading and high strains, evolution has adapted the structure such that presumably there is no advantage for housing and maintaining living osteocytes. Such adaptation is also seen in other fish [2, 22]. We propose that the pivot of the cleithrum well sustains the loading scenarios imposed on it (Fig. 1) due to the microscopic layering and the macroscopic oval geometry, and that the structural features that we observed provide a reasonably optimized mechanical advantage compared to other cell

containing (osteocytic) structures usually seen in mammalian bone. Bones are known to heal and adapt [23], and evidently, the cleithra of pike are no different [2]. The microstructure adapts by adding material in layers and by partial removal and enlargement of internal cavities. We speculate that cells such as osteoblasts and osteoclasts, present on the internal and external surfaces sense the state of strain in the bone bulk by an as yet unknown mechanism. Cells in the cavities must direct the addition or removal of material [24] to adapt the bone geometry. Further research is needed to know how this is achieved.

By combining methods to map the mineral, collagen and the intact structure (SEM, SHG and phase contrast-enhanced μCT) we revealed a cross-linked network of fibers, bound together to create an impressive tough structure. The varying degrees of mineral density observed in adjacent layers probably helps to toughen these bones [25]. Local variations in the orientation of the mineralized collagen fibers further help to tune both stiffness and resistance to damage. Indeed undulating layers pinned by fibers are very difficult to separate and crack, making the structure excellently resistant to damage propagation [25, 26]. This suggests that there are alternatives to housing living cells (osteocytes) for excellent bone maintenance and management of structural integrity, but these may be limited to specific repeated loading scenarios and not to unspecific incoming mechanical loading scenarios that are common in mammals. This suggests that these fish bones are highly tuned to match the mechanical demands. Collagen fibers in the outer regions appear to be thinner as compared to the fibers at the center of the samples, as shown in the color change from green to yellow to orange to red in Fig. 3d [10].

In summary, we find that the cleithrum bones are made of long vast arrays of parallel mineralized collagen fibers, comprising pinned composite layers devoid of cells. They contain large internal cavities and are surrounded with a dense cortex. The reason for this regional difference is not known, however, it is seen consistently in all cortical areas observed in cross-section. Further work is needed to better understand this finding. Such an internal architecture could be an inspiration for flexible and mechanically damage-resistant biomimetic materials.

We acknowledge the ESRF (European Synchrotron Radiation Facility (ID19), Grenoble, France) for beamtime. We thank Gabriela Korus for help and fruitful discussions during histological sample preparation. This research partially supported by the German Israeli Foundation (GIF) grant I-1278 and by a student grant of the Berlin-Brandenburg School for Regenerative Therapies (BSRT), Berlin, Germany.

References

[1] A. Atkins, J. Milgram, S. Weiner, R. Shahar: J. Exp. Biol. 218 (2015) 3559. DOI:10.1242/jeb.124073.
[2] A. Atkins, M.N. Dean, M.L. Habegger, P.J. Motta, L. Ofer, F. Repp, A. Shipov, S. Weiner, J.D. Currey, R. Shahar: Proc. Natl. Acad. Sci. U.S.A. 45 (2014) 1647. DOI:10.1073/pnas.1412372111.
[3] M. Jollie: J. Morphol. 147 (1975) 61. DOI:10.1002/jmor.1051470106.
[4] F. Scharf, R. Yetter, A. Summers, F. Juanes: Fish. Bull. 96 (1998) 575.
[5] http://palaeos.com/vertebrates/euteleostei/esociformes3.html.
[6] J.W.M. Elshoud-Oldenhave: Zoomorphol. 93 (1979) 1. DOI:10.1007/BF02568672.
[7] N. Konow, C.P.J. Sanford: J. Exp. Biol. 211 (2008) 3378. DOI:10.1242/jeb.023564.
[8] M.D. Faust, J.J. Breeggemann, S. Bahr, B.D.S. Graeb: J. Fish Wildl. Manag. 4 (2013) 332. DOI:10.3996/062013-JFWM-041.
[9] A.O. Laine, W.T. Momot, P.A. Ryan: N. Am. J. Fish Manag. 11 (1991) 220. DOI:10.1577/1548-8675(1991)011<0220:AOUSAC>2.3.CO;2.
[10] L. Rich, P. Whittaker: Braz. J. Morphol. Sci. 22 (2005) 97.
[11] J.D. Currey. "Bones – Structure and Mechanics": Princeton University Press, New Jersey. (2002).
[12] T.G. Bromage, H.M. Goldman, S.C. McFarlin, J. Warshaw, A. Boyde, C.M. Riggs: Anat. Rec. B: N. Anat. 274B (2003) 157. DOI:10.1002/ar.b.10031.
[13] A. Ascenzi, E. Bonucci: Anat. Rec. B: N. Anat. 158 (1967) 375. ar.1091580403. DOI:10.1002/
[14] A. Ascenzi, E. Bonucci: Anat. Rec. 161 (1968) 377. 1002 / ar. 1091610309. DOI:10
[15] A. Ascenzi, E. Bonucci: J. Biomech. 19 (1986) 455. . 1016 / 0021 – 9290(86)90022 – 9. DOI:10
[16] D. Paganin, S.C. Mayo, T.E. Gurreyev, P.R. Miller, S.W. Wilkins: J. Microsc. 206 (2002) 33. DOI:10.1046/j.1365-2818.2002.01010.x.
[17] A. Mirone, E. Gouillart, E. Brun, P. Tafforeau, J.Kieffer: Nucl. Instrum. Methods Phys. Res. B. 324 (2014) 41. DOI:10.1016/j.nimb.2013.09.030.
[18] I. Zlotnikov, V. Schoeppler: Adv. Funct. Mater. 27 (2017) 1. DOI:10.1002/adfm.201700506.
[19] C. Schneider, W. Rasband, K. Eliceiri: Nat. Methods. 9 (2012) 671. DOI:10.1038/nmeth.2089.
[20] L.C.U. Junqueira, G. Bignolas, R.R. Brentani: Histochem J. 11 (1979) 447. DOI:10.1007/BF01002772.
[21] M. Walker, R.E. Smith: Compos. Struct. 62 (2003) 123. DOI:10.1016/S02638223(03)00098-9.
[22] A. Atkins, N. Reznikov, L. Ofer, A. Masic, S.Weiner, R. Shahar: Acta Bio-mater. 13 (2015) 311. DOI:10.1016/j.actbio.2014.10.025.
[23] J.D. Currey: J. Biomech. 36 (2003) 1487. .1016 /S0021 – 9290(03)00124 – 6. DOI:10
[24] M.B. Schaffler, O.D. Kennedy: Curr. Osteoporos. Rep. 10 (2012) 118. DOI:10.1007/s11914-012-0105-4.
[25] P. Fratzl, O. Kolednik, F.D. Fischer, M.N. Dean: Chem. Soc. Rev. 45 (2016) 252. DOI:10.1039/C5CS00598A.
[26] O. Kolednik, J. Predan, F.D. Fischer, P. Fratzl: Acta Mater. 68 (2014) 279. DOI:10.1016/j.actamat.2014.01.034.

(Received October 25, 2018; accepted March 23, 2019; online since November 19, 2019)

Correspondence address

Katrein Sauer
Paul Zaslansky
JWI Julius Wolff Institut
Charité – Universitätsmedizin Berlin
Föhrerstr. 15
13535 Berlin
Germany
Tel.: (+49) 30 450 559 217
E-mail: katrein.sauer@gmail.com
E-mail: paul.zaslansky@charite.de

Bibliography
DOI 10.3139/146.111801
Int. J. Mater. Res. (formerly Z. Metallkd.)
111 (2020) 1; page 78 – 85

ISSN 1862-5282